

Chapter 2

Classical Optical Interferometry for Strain Measurement

Nils G. Ohlson

Abstract Paper describes measurement of displacements and strains under environmental circumstances which have necessitated development of special techniques based on elementary optical interferometry. Examples are given of measurements at high temperature, high strain rate, and small deformations. Emphasis is on simplicity in the experimental set-up as well as in evaluation of tests. It is concluded that the methods described may be useful at times, as results can be obtained despite difficult circumstances although the resolution might be somewhat limited.

2.1 Introduction

In spite of the huge development of advanced optical methods for measuring purpose that we are currently witnessing, it may sometimes be worth-while returning to basics. Experiments involving measurements of strains and displacements can be arranged by reconsidering elementary laws of physics. Such approach can be advantageous, since it only requires use of simple and less expensive equipment. Tests may also be easily evaluated. Limited resolution and rather high measuring errors, however, are disadvantages that should not be concealed. Pointwise measurements instead of full-field display of results is can also become a limitation.

In this paper, focus will be on the equipment required. Results of tests will only be outlined briefly but reference is made to different papers where they have been subject to comprehensive discussions.

2.2 Measuring Strains at High Temperature

The test described dates back to the middle of the 1960s. Gas lasers had recently become commercially available. In order to study the behavior of metal alloys subjected to a thermally induced cyclic load, a wedge-shaped bar was heated along its edge by means of an inductive coil placed close to the edge, Fig. 2.1. Each load cycle comprised a period of heating followed by some cooling. The cycle should simulate what is encountered by turbine blades in an aircraft engine. Cracks begin to develop in the specimen. It was desired to correlate the number of cycles to crack initiation with the strains generated on the specimen surface.

Materials tested were Nimonic alloys and tool steels. Tests were performed in a vacuum chamber. Maximum temperature was of the order of 800°C. A diffraction grating was applied to the polished surface mechanically. Scratching the surface with a diamond pyramid, of the kind that is used for microhardness testing, under low contact force (5 g) in a “microcutter” (Leppin & Masche, Berlin), fitted with a precision screw for obtaining sidewise displacement between grooves, gave a reflection grating, having 50 lines per mm, Fig. 2.2. Illumination by a 5 mW HeNe laser beam allowed for observation of ten diffracted beams on either side of the center reflection. Resolution of strains of about 100 microstrains was achieved. The diffraction angle Θ_n for the n :th beam satisfies the relation

$$\sin \Theta_n = n\lambda/d \quad (2.1)$$

N.G. Ohlson (✉)

Solid Mechanics Department, The Royal Institute of Technology, Stockholm SE-100 44, Sweden

e-mail: ngohlson@kth.se

Fig. 2.1 Specimen used for thermal fatigue tests, mechanical grating on surface

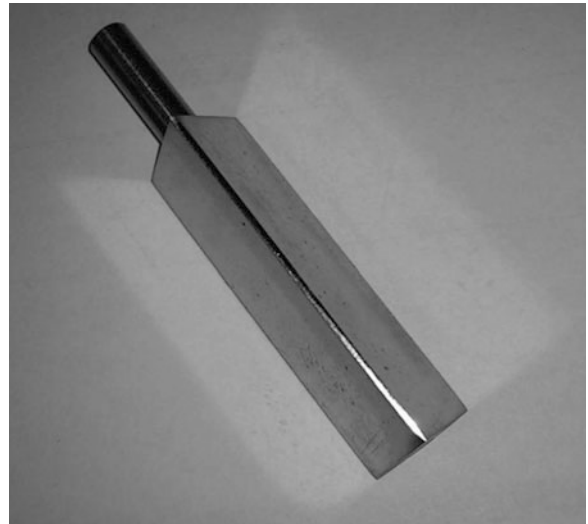
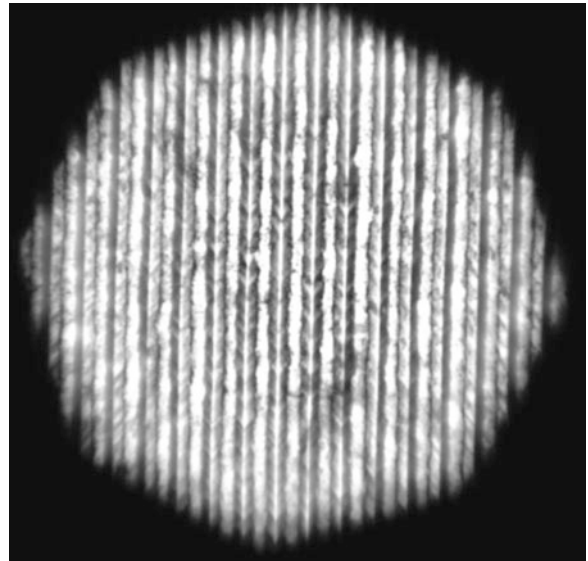


Fig. 2.2 Microphoto of mechanical grating, produced by scratching, $d = 0.02$ mm



where λ denotes the wave length and d equals the distance between grooves of the grating.

The mechanically manufactured grating was chosen because of the harsh environment in the thermal fatigue test. Needless to say, better resolution will be obtained with gratings of higher density and also of better precision, namely, concerning the grating parameter. Such gratings can be applied by etching the metal surface after it has been covered with a mask of photographically deposited silver, copied onto the surface in a camera-like set-up in front of it. As an alternative to analyzing the grating by pointwise illumination with the laser beam in real time, it was possible to produce a photo of the deformed grating and analyze the photographic plate point by point, thus mapping the strain in one direction at the time that the photo was taken, across the whole area covered by grating.

Results are shown in Fig. 2.3 for a set of points of measurement ranging from the edge and in a direction perpendicular to it. Curves show longitudinal strain versus time. Maximum value of strain in the point close to the edge (red curve) was 1.12%. Cycling time was 30 s. Temperature recordings were done simultaneously, using the emitted infra-red radiation for exposure of a photographic plate and ensuing density measurements of the exposed and developed emulsion. Test results are described in [1].

For an amateur scientist, a high-quality reflection grating is available at almost no cost in the form of a piece cut out from a standard compact disc and then bonded to the specimen. Resolution of the order of 10 microstrains is readily obtained by direct projection of the first order reflections on a screen situated a few yards from the specimen.

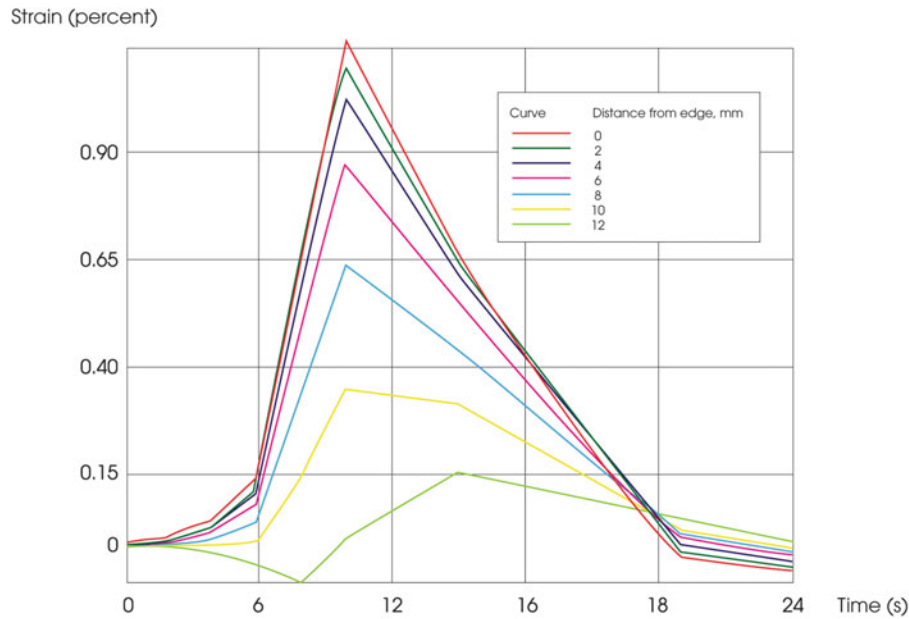


Fig. 2.3 Longitudinal strain for some points on specimen surface versus time. Top curve for point near the edge. The curves below are for points in order from the edge according to legend in the diagram. Total cycle time 30 s, maximum strain 1.12%

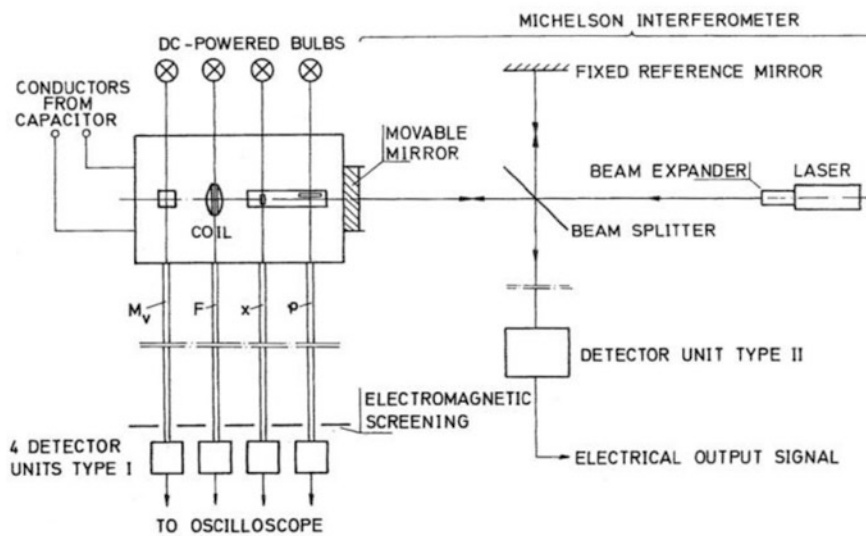


Fig. 2.4 Principal arrangement of measuring equipment for biaxial high-speed testing machine, interferometer to the right

2.3 Measuring Displacements at High Loading Rates

A tensile testing machine was designed based on the principle that tensile force may be obtained between induction coils, coaxially arranged, by discharging a set of high-voltage capacitors through one of the coils, [2]. Small specimens were used (2.6 mm diameter, 5 mm length). Even torsional moment was obtainable in this machine. Since high electromagnetic fields are created due to the discharge, electronic equipment was considered unsuitable for recording test parameters. Instead, a Michelson interferometer was built for measuring the elongation of the specimen whose one end was attached to one of the mirrors of the interferometer, Fig. 2.4. The motion of this mirror was monitored by a photo-diode, which recorded a pulse train as the optical path length changed with time. Figure 2.5 shows the original pulse train A, which after due modification

Fig. 2.5 Pulse train on its way through electronic device: at photo diode *A*, after triggering unit *A'*, at pulse counter *B*, final integrated displacement signal *C*

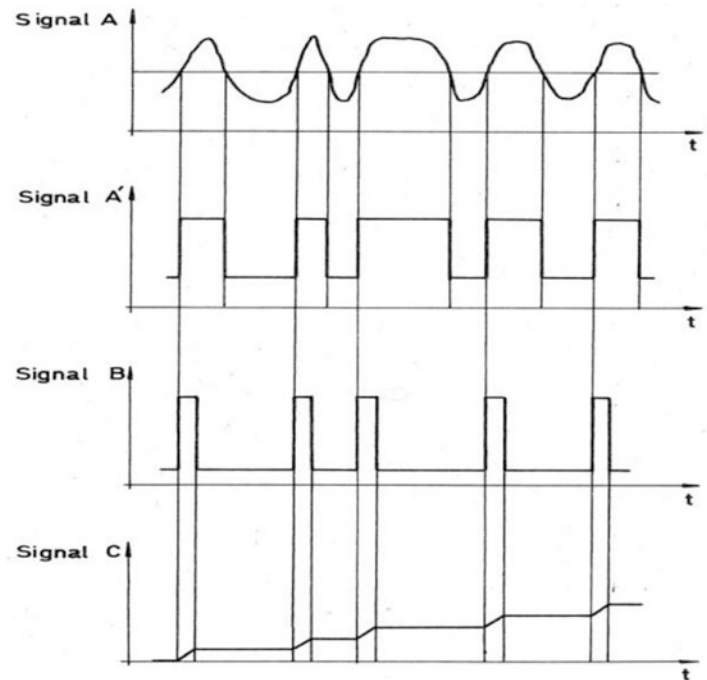
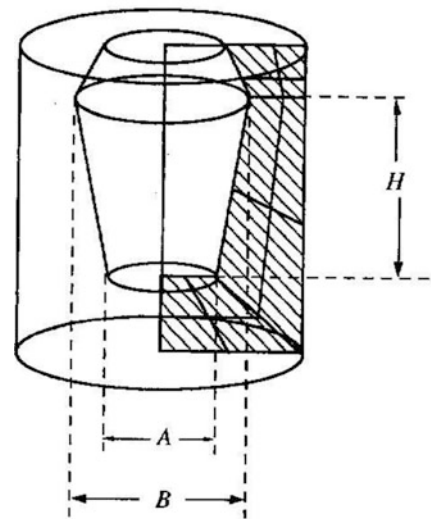


Fig. 2.6 Model of prepared tooth after grinding, for upper jaw



resulted in the displacement signal *C*. Pulse lengths, corresponding to optical fringes passing past the diode, of the order of 200 μ s were recorded, although the rise time of the equipment was as low as 0.5 ns and its recovery time 0.6 ns.

2.4 Measuring Stresses in Photoelasticity

In prosthetic dentistry, a fairly complicated preparation procedure is required prior to the final attachment of artificial crowns and bridges in the patient's mouth. This procedure involves transforming the tooth into an abutment, making reprints of it by use of impression materials, pouring the gypsum model and finally casting the crown which is then to fit the abutment with high precision. A typical abutment is shown in Fig. 2.6. For the purpose of studying the influence of selection of impression material, of abutment angles, and of shrinkage of the cast structure on the precision of the crown, an investigation was

Fig. 2.7 Isochromatic fringes from photoelastic test of artificial crown model

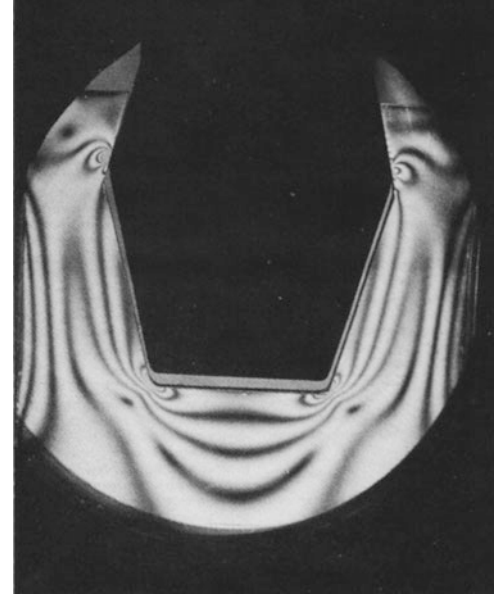
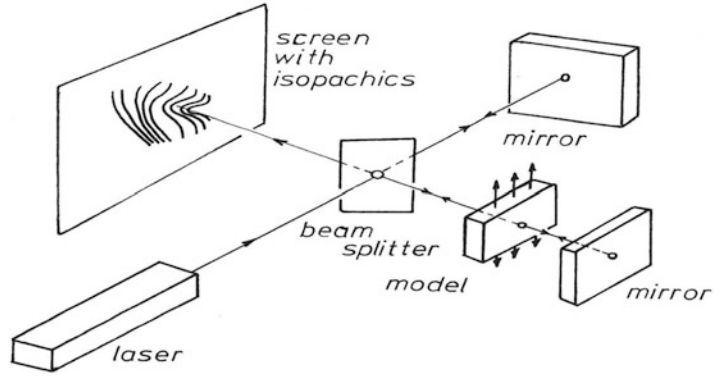


Fig. 2.8 Interferometer arrangement for measuring thickness changes of photoelastic model



undertaken, combining experimental work on a model with numerical evaluation of all steps in the procedure mentioned above, [3].

For investigating effect of the cone angles, a two-dimensional model of the crown was manufactured from a photoelastic material. The isochromatic fringe pattern shown in Fig. 2.7 displays curves for constant principal stress difference, as is well-known from elementary theory of photoelasticity. One has

$$\sigma_1 - \sigma_2 = m\lambda/tc \quad (2.2)$$

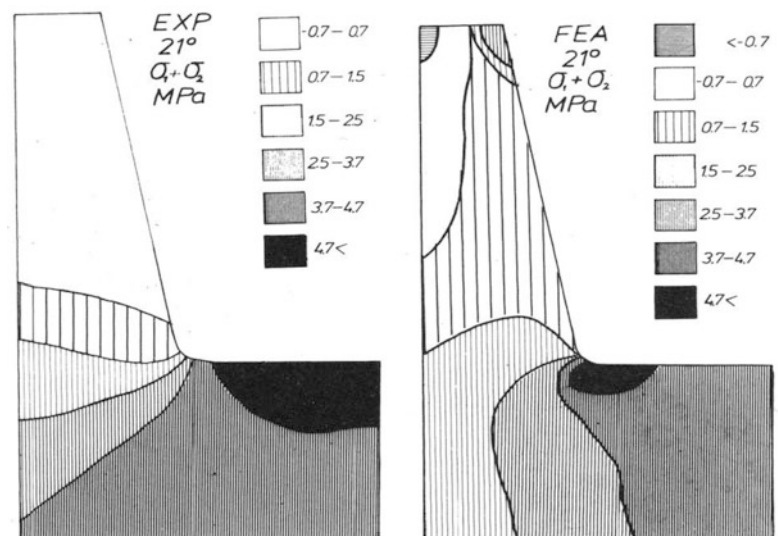
where t denotes the thickness of the model, c is a photoelastic material parameter and m any integer, positive or negative, or zero.

A simple way of simultaneous measuring the sum of the principal stresses can be obtained by inserting the transparent model into the measuring beam of the above-mentioned Michelson interferometer, Fig. 2.8. The thickness changes in the model are directly proportional to this sum and are also related to the change in optical path length in the active beam of the interferometer. Hooke's law directly gives

$$\frac{\Delta t}{t} = \varepsilon_3 = -\left(\frac{\nu}{E}\right)(\sigma_1 + \sigma_2) = \frac{2m-1}{4(N-1)}\left(\frac{\lambda}{t}\right) \quad (2.3)$$

where N denotes the index of refraction of the model material.

Fig. 2.9 Comparison of result from thickness measurement according to Fig. 2.8 (EXP) and finite element analysis (FEA)



Thus, bright and dark fringes will appear in the plane where the photo detector is situated. The number of fringes counted in a certain point of the model is then proportional to the sum of these stresses, assuming that the applied load is known. The practical determination of this number is rather difficult. Instead of aligning the interferometer mirrors in a perfect manner, one may allow for some tilt. This results in a fringe pattern which exists even for zero load on the model. Upon application of load, correct fringe number may be obtained starting the count from a point on the boundary of the model in which the sum equals zero. – The state of stress can be evaluated completely from the two sets of fringes. An example of results achieved is shown in Fig. 2.9, where experimental results are compared with those received by finite element analysis.

2.5 Measuring Small Displacements

Because of its high resolution, which is of the order of half a wavelength of light, the interferometer lends itself very well to measuring small displacements. A test was performed which aims at deterring the stiffness of a microscopic alga when subjected to uniaxial compression, similar to what is achieved in layers of silt where algae are embedded as they are deposited at the bottom in a river mouth. Such deposits may become mineralized (“petrified”) and remain as three-dimensional fossils over millions of years. The presence in a silt sample of certain species of algae (or spores or pollen grains) may indicate prospective occurrence of mineral oil or natural gas and is therefore important. The deformation of these micro-organisms while they are still fresh depends on the properties of the species and on the compaction pressure they are encountering during the deposition.

Figure 2.10 shows SEM photographs of cysts of species *Tasmanites*, appearing as almost spherical shells (diameter 60 μm , approximately), from the Middle Jurassic, [4]. Modern day relatives of the same genus were subjected in our test to compression between glass plates and the relationship between force and deformation recorded, [5]. The interferometer was similar to the ones described previously. A specially designed device was used for applying load on the algae, Fig. 2.11. Three such spheres were placed between the glass plates, one of these plates consisting of the mirror of the interferometer. Since the samples are immersed in a drop of water, the optical path length is reduced, as the samples are compressed. Interference fringes passing the detector are counted.

Load is increased by placing small weights on the sample device. Attention must be paid to the surface tension of the droplet, either by compensating for it (requires knowledge of its diameter) or by immersion of the whole mirror into water. Springs surrounding the platform were used for balancing the mass of platform shown in the figure.

It was discovered that the stiffness of the algae depends on their age, the older the stiffer. Their lifecycle is of the order of a few months. If the average size was 120 μm , a load of 2 N resulted in a 2 μm compression, approximately.

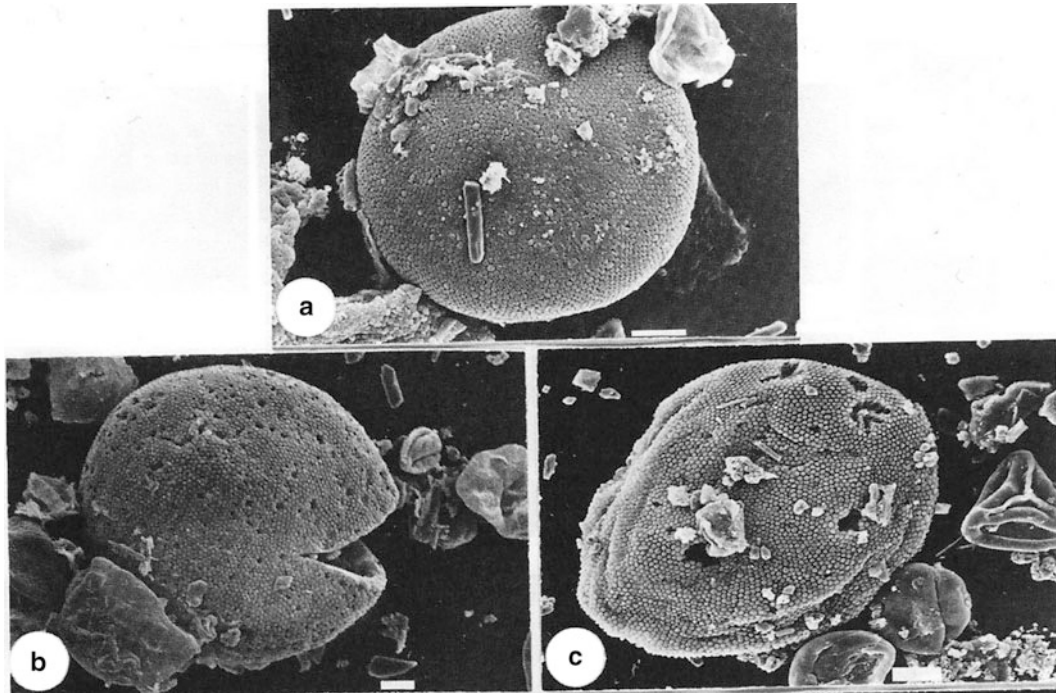


Fig. 2.10 Microfossil of species *Tasmanites*: undamaged sample (*top*), sample with crack (*bottom left*), sample with folds (*bottom right*). White bar denotes length 10 μm



Fig. 2.11 Experimental device for the compression of samples according to Fig. 2.10, for use in interferometer for recording deformation. Samples placed on round glass surface in the middle, to be covered by interferometer mirror

2.6 Discussion

If modern commercial optical testing equipment for determining strains is available it is so powerful that it seldom pays trying to replace it by building your own experimental set-up. Examples above show that it does pay, however, provided that the demands are somewhat off main-stream. When interferometric experiments are performed, high precision in alignment of components is required. Measurements by means of gratings must be compensated for changes in the normal direction of

the specimen surface, which may be done by monitoring several interference fringes, including the zero order reflexion, simultaneously. Pulse counting methods has the advantage of avoiding the scatter in analogous measurements which improves resolution.

References

1. Odqvist FKG, Ohlson NG (1968) Thermal fatigue and thermal shock investigations. In: Boley BA (ed) Thermoelasticity. Springer, 1970, IUTAM symposium, East Kilbride, pp 188–205
2. Ohlson NG (1974) A high-speed testing machine for biaxial states of stress. *Rev Sci Instrum* 45:827–833
3. Ohlson NG, Pamenius M (1988) Optical methods for complete stress determination – an experimental alternative to finite-element analysis. *Mater Des* 9:155–164
4. Guy-Ohlson D, Ohlson NG, Lindqvist B (1988) Fossil palynomorph deformation and its relationship to sedimentary deposition. *Geologiska Föreningens i Stockholm Förhandlingar* 110:111–119
5. Ohlson NG, Guy-Ohlson D (1995) An optical interferometric method for the measurement of microdeformation in sediments. *J Sediment Res* 65:572–574

Imaging Methods for Novel Materials and Challenging
Applications, Volume 3

Proceedings of the 2012 Annual Conference on
Experimental and Applied Mechanics

Jin, H.; Sciammarella, C.; Furlong, C.; Yoshida, S. (Eds.)

2013, X, 450 p., Hardcover

ISBN: 978-1-4614-4234-9